Electronic Supplementary Material

Passivation Principle of Deep-Level Defect: A Study of Sn_{Zn} Defect in Kesterites for High-Efficient Solar Cells

Ke Zhao,[a,b] Huiwen Xiang,[a] Rui Zhu,[a] Chengyan Liu,*[a] Yu Jia[a,b]

[a]Key Laboratory for Special Functional Materials of Ministry of Education, The Joint Center for Theoretical Physics, Collaborative Innovation Center of Nano Functional Materials and Applications, and School of Materials Science and Engineering, Henan University, Kaifeng, Henan 475001, China.

[b]International Laboratory for Quantum Functional Materials of Henan, and School of Physics and Microelectronics, Zhengzhou University, Zhengzhou 450001, China

I. Energy levels

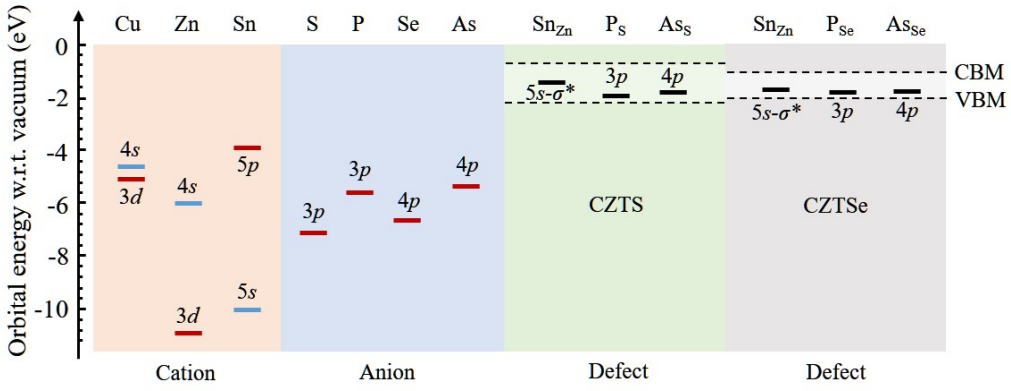

Fig. S1 Schematic diagram of cations (Cu, Zn and Sn) and anions (S, P, Se and As) atomic energy levels and defects (Sn_{Zn}, P_S, P_{Se}, As_S and As_{Se}) levels referencing to the vacuum level.

Table S1. Atomic orbital energy levels of valence electrons and defect levels relative to vacuum energy level.

Atom/ Defect	Electronic configuration	Valence electron	Energy ref. to vacuum (eV)	2nd highest Energy orbital	Energy ref. to vacuum (eV)
Cu	$[Ar]3d^{10}4s^1$	4*s*	-4.682	3*d*	-5.504
Zn	$[Ar]3d^{10}4s^2$	4*s*	-6.060	3*d*	-10.855
Sn	$[Kr]4d^{10}5s^25p^2$	5*p*	-3.930	5*s*	-10.050
S	$[Ne]3s^23p^4$	3*p*	-7.120	--	--
P	$[Ne]3s^23p^3$	3*p*	-5.607	--	--
Se	$[Ar]3d^{10}4s^24p^4$	4*p*	-6.689	--	--
As	$[Ar]3d^{10}4s^24p^3$	4*p*	-5.374	--	--
Sn_{Zn} in CZTS	--	--	-1.458	--	--
P_S	--	--	-1.934	--	--
As_S	--	--	-1.864	--	--

Sn_{Zn} in CZTSe	--	--	-1.994	--	--
P_{Se}	--	--	-2.164	--	--
As_{Se}	--	--	-2.144	--	--

II. First-principles calculation method

The first-principles density functional theory (DFT) is used to perform the calculations by using the Vienna *Ab initio* Simulation Package (VASP).[1,2] The projector-augmented-wave (PAW) method with the Perdew-Burke-Ernzerhof (PBE) functional of the generalized gradient approximation (GGA) is used to all the structural relaxation. Generally, GGA presents a more reliable result for defect system than that of local density approximation (LDA), owing to its great description of a system with a large fluctuation of charge density. The energy cutoff is 350 eV and the Hellmann-Feynman force is less than 1×10^{-3} eVÅ^{-1}. All the defect models are constructed based on a $2 \times 2 \times 2$ supercell including 64 atoms by extending the fully relaxed Cu_2ZnSnS_4 (CZTS) unit cell with the lattice constants of a = b = 5.466 Å and c = 10.931 Å. A larger $3 \times 3 \times 2$ supercell is examined to calculate the electronic structures and formation energies of defect systems, and the similar results are obtained. Subsequently, defect model created based on the perfect supercell are fully relaxed under the fixed lattice constants. K-points are sampled with $6 \times 6 \times 3$ and $3 \times 3 \times 3$ meshes in the Brillouin zone for the calculations of unit cell and defect systems, respectively. All the energies used in the calculations of defects' formation energies and phase diagram are derived from the hybrid exchange-correlation functional (HSE06)[3,4] based on the PBE fully relaxed structures. The exchange parameter of 0.30 is used to adjust the calculated bandgap of CZTS to the experimental value (1.51 eV).[5] The band structures are calculated by using Hubbard U = 6.0 eV on the cation 3d orbital,[6,7] which leads to the bandgap of 0.73 eV in CZTS bulk.

III. Band structures of Cu_2ZnSnS_4

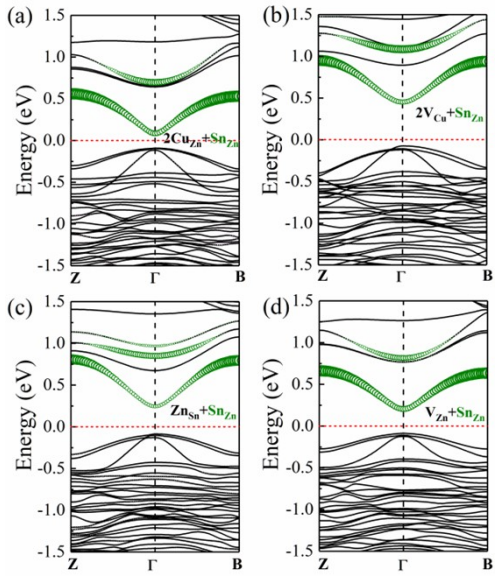

Fig. S2 Band structures of (a) $2Cu_{Zn}+Sn_{Zn}$, (b) $2V_{Cu}+Sn_{Zn}$, (c) $Zn_{Sn}+Sn_{Zn}$ and (d) $V_{Zn}+Sn_{Zn}$ defect complexes weighted by the contribution of Sn_{Zn} defect colored by green circles. The deep-level caused by Sn_{Zn} defect still exists in the Sn_{Zn} related intrinsic defect complexes.

IV. Band structures of $Cu_2ZnSnSe_4$

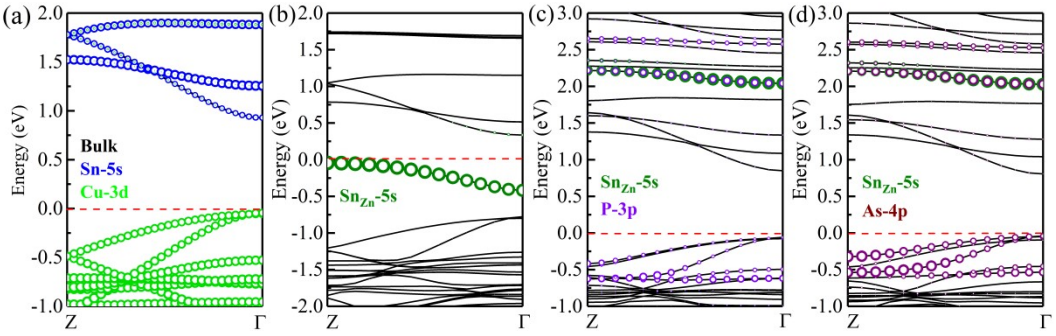

Fig. S3 Band structures for $Cu_2ZnSnSe_4$ (CZTSe) system by the HSE06 calculations. (a) Defect-free CZTSe supercell. The CBM and VBM originate from the antibonding state of Sn-5s/Se-4p and Cu-3d/Se-4p, respectively. (b) Isolated Sn_{Zn} defect. The Sn_{Zn} defect induces a defect level within the bandgap weighted by green cycles in energy band. (c) $2P_S+Sn_{Zn}$ defect complex. (d) $2As_{Se}+Sn_{Zn}$ defect complex. Both of two P_S defects and two As_{Se} defects associating with the Sn_{Zn} defect can successfully passivate the defect level caused by Sn_{Zn} defect.

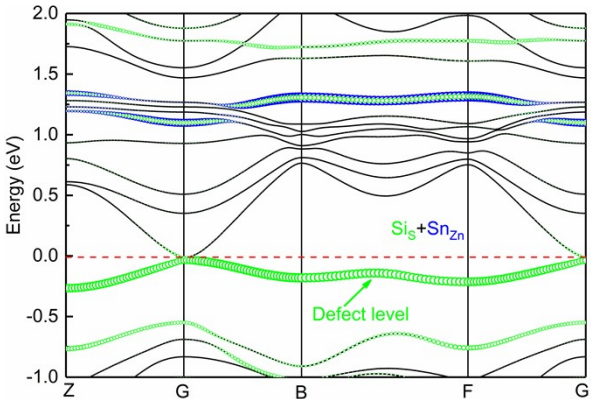

Fig. S4 Band structure of Si_S+Sn_{Zn} defect complex system by DFT+U calculations. The blue and the green circles represent the contribution of Si_S-3p and Sn_{Zn}-5s orbitals, respectively.

V. Phase diagram

Since the formation energy of defect is a functional of elemental chemical potential, phase diagram is calculated to limit the region of elemental chemical potentials. CZTS phase diagram is thermodynamically constrained by the following conditions. The first is as follow:

$$\mu_X \le 0, (X = \text{Cu, Zn, Sn, S and P}) \tag{1}$$

is used to avoid the pure phases of Cu, Zn, Sn, S and P during the production of CZTS with P incorporation. To obtain the CZTS host, the chemical potentials of Cu, Zn, Sn and S should satisfy the following equation:

$$2\mu_{\text{Cu}} + \mu_{\text{Zn}} + \mu_{\text{Sn}} + 4\mu_{\text{S}} = \Delta H_{\text{Cu}_2\text{ZnSnS}_4}\ (-4.82\ \text{eV}) \tag{2}$$

To avoid the formation of secondary phases, such as Cu_2S ($P2_1/c$), Cu_2SnS_3 (Cc), CuS (Cmcm), $CuSn_4S_8$ ($F\bar{4}3m$), Sn_2S_3 (Pnma), SnS (Pnma), SnS_2 ($P\bar{3}m1$), ZnS ($F\bar{4}3m$) and $ZnSnS_3$ (R3c), their formation enthalpies should satisfy the following inequations:

$$\begin{aligned}
&2\mu_{\text{Cu}} + \mu_{\text{S}} \le \Delta H_{\text{Cu}_2\text{S}}\ (-0.89\ \text{eV}) \\
&2\mu_{\text{Cu}} + \mu_{\text{Sn}} + 3\mu_{\text{S}} \le \Delta H_{\text{Cu}_2\text{SnS}_3}\ (-2.66\ \text{eV}) \\
&\mu_{\text{Cu}} + \mu_{\text{S}} \le \Delta H_{\text{CuS}}\ (-0.53\ \text{eV}) \\
&\mu_{\text{Cu}} + 2\mu_{\text{S}} \le \Delta H_{\text{CuS}_2}\ (-0.22\ \text{eV}) \\
&\mu_{\text{Cu}} + 4\mu_{\text{Sn}} + 8\mu_{\text{S}} \le \Delta H_{\text{CuSn}_4\text{S}_8}\ (-5.05\ \text{eV}) \\
&2\mu_{\text{Sn}} + 3\mu_{\text{S}} \le \Delta H_{\text{Sn}_2\text{S}_3}\ (-2.12\ \text{eV}) \\
&\mu_{\text{Sn}} + \mu_{\text{S}} \le \Delta H_{\text{SnS}}\ (-0.86\ \text{eV}) \\
&\mu_{\text{Sn}} + 2\mu_{\text{S}} \le \Delta H_{\text{SnS}_2}\ (-1.29\ \text{eV}) \\
&\mu_{\text{Zn}} + \mu_{\text{S}} \le \Delta H_{\text{ZnS}}\ (-1.96\ \text{eV}) \\
&\mu_{\text{Zn}} + \mu_{\text{Sn}} + 3\mu_{S} \le \Delta H_{\text{ZnSnS}_3}\ (-2.34\ \text{eV})
\end{aligned} \tag{3}$$

Considering the P doping with the maximum allowed potential, the P related secondary phases, such as Cu_4SnP_{10} (R3m), CuP_2 ($P2_1/c$), $CuPS_3$ ($P4_2/mnm$), Sn_4P_3 (R $\bar{3}$ m), $SnPS_3$ (P_c), $Zn_3P_2S_8$ (P $\bar{4}$ n2), ZnP_2 ($P4_32_12$) and $ZnSnP_2$ (I $\bar{4}$ 2d) should be avoiding by satisfying the following inequations:

$$\begin{aligned}
&4\mu_{Cu} + \mu_{Sn} + 10\mu_P \le \Delta H_{Cu_4SnP_{10}} \left(-2.58\ \text{eV}\right) \\
&\mu_{Cu} + 2\mu_P \le \Delta H_{CuP_2} \left(-0.55\ \text{eV}\right) \\
&\mu_{Cu} + \mu_P + 3\mu_S \le \Delta H_{CuPS_3} \left(-1.65\ \text{eV}\right) \\
&4\mu_{Sn} + 3\mu_P \le \Delta H_{Sn_4P_3} \left(-1.53\ \text{eV}\right) \\
&\mu_{Sn} + \mu_P + 3\mu_S \le \Delta H_{SnPS_3} \left(-1.91\ \text{eV}\right) \\
&3\mu_{Zn} + 2\mu_P + 8\mu_S \le \Delta H_{Zn_3P_2S_8} \left(-7.40\ \text{eV}\right) \\
&\mu_{Zn} + 2\mu_P \le \Delta H_{ZnP_2} \left(-0.92\ \text{eV}\right) \\
&\mu_{Zn} + \mu_{Sn} + 2\mu_P \le \Delta H_{ZnSnP_2} \left(-0.99\ \text{eV}\right)
\end{aligned} \tag{4}$$

VI. Defect's formation energy

The formation energy of defect $\Delta H\left(\alpha, q\right)$ is expressed as follows:[8]

$$\Delta H\left(\alpha, q\right) = \Delta E\left(\alpha, q\right) + n_{Cu}\mu_{Cu} + n_{Zn}\mu_{Zn} + n_{Sn}\mu_{Sn} + n_S\mu_S + n_P\mu_P + qE_F, \tag{5}$$

$$\Delta E\left(\alpha, q\right) = E\left(\alpha, q\right) - E\left(host, 0\right) + n_{Cu}\mu_{Cu}^0 + n_{Zn}\mu_{Zn}^0 + n_{Sn}\mu_{Sn}^0 + n_S\mu_S^0 + n_P\mu_P^0 + qE_{VBM}, \tag{6}$$

where $E\left(\alpha, q\right)$ is the total energy of a defect α with charge state *q* in a supercell model. E_F is the Fermi energy level relative to the VBM of CZTS host (E_{VBM}). $E\left(\text{host}, 0\right)$ is the total energy of neutral CZTS host with the same supercell as defect model. n_i is the difference in the number of element *i* between host and the defect system.

VII. The chemical potentials at extreme points

Table S2. The values of elemental chemical potentials at all the extreme points of CZTS phase diagram with P doping.

	μ_{Cu} (eV)	μ_{Zn} (eV)	μ_{Sn} (eV)	μ_{S} (eV)	μ_{P} (eV)
A	-0.69	-2.15	-1.29	0.00	-0.96
B	-0.79	-1.96	-1.29	0.00	-0.86
C	-0.57	-1.53	-0.42	-0.43	-0.19
D	-0.47	-1.72	-0.42	-0.43	-0.19
E	-0.05	-1.30	0.00	-0.85	-0.25
F	-0.15	-1.10	0.00	-0.85	-0.20
G	0.00	-1.01	0.00	-0.95	-0.28
H	0.00	-1.07	-0.19	-0.89	-0.28
J	0.00	-1.27	0.00	-0.88	-0.27
K	-0.36	-1.99	-1.45	-0.16	-0.80
L	-0.36	-1.80	-1.65	-0.16	-0.80
M	-0.53	-1.96	-1.81	0.00	-1.12
N	-0.53	-2.15	-1.61	0.00	-1.12
O	-0.53	-1.49	-0.38	-0.47	-0.11
P	-0.46	-1.52	-0.35	-0.50	-0.04
Q	-0.49	-1.51	-0.53	-0.45	-0.03
R	-0.06	-1.27	0.00	-0.86	-0.24
S	0.00	-1.22	0.00	-0.90	-0.28
T	-0.06	-1.18	-0.42	-0.78	-0.25

References

1 G. Kresse and J. Hafner, *Phys. Rev. B*, 1993, **47**, 558–561.

2 G. Kresse and J. Hafner, *Phys. Rev. B*, 1994, **49**, 14251–14269.

3 S.-H. Wei and A. Zunger, *Appl. Phys. Lett.*, 1998, **72**, 2011–2013.

4 S.-H. Wei and A. Zunger, *Phys. Rev. Lett.*, 1987, **59**, 144–147.
5 J. Seol, S. Lee, J. Lee, H. Nam and K. Kim, *Solar Energy Materials and Solar Cells*, 2003, **75**, 155–162.
6 J. P. Perdew and Y. Wang, *Phys. Rev. B*, 1992, **45**, 13244–13249.
7 S. L. Dudarev, G. A. Botton, S. Y. Savrasov, C. J. Humphreys and A. P. Sutton, *Phys. Rev. B*, 1998, **57**, 1505–1509.
8 S.-H. Wei and S. B. Zhang, *Phys. Rev. B*, 2002, **66**, 155211.